gmfELUCIDATING CHEMOTHERAPEUTIC DRUG TRANSPORT OF DIFFERENT AGENTS AND OF ANTIOANGIOGENIC THERAPY AGAINST A BRAIN TUMOR

Davis Yohanes Arifin, MEBCS, Singapore-MIT Alliance, 4 Engineering Drive 3, Singapore 117576
Kam Yiu Timothy Lee, Gleneagles Hospital Ltd, 6A Napier Road, Singapore 25850
Chi-Hwa Wang, Department of Chemical and Biomolecular Engineering, National University of Singapore, 4 Engineering Drive 4, Singapore, 117576
Kenneth A. Smith, Department of Chemical Engineering, Massachusetts Institute of Technology, Cambridge, MA 02139

Introduction

Treatment against brain tumors usually involves surgical removal, chemotherapy, and radiotherapy. For chemotherapy, the first FDA-approved treatment is the Gliadel® wafer (1). This wafer is able to provide sustained release of *carmustine* locally to the remnant tumor. However, results have been highly variable due to the significant loss of *carmustine* to blood capillaries, resulting in a limited (millimeter) penetration distance (2). This suggests that the cause of poor performance for this drug delivery device is related to the drug transport mechanism in the tumor tissue, not the local delivery concept.

The above example shows how drug transport properties are often overlooked. Though the drug is clinically effective against the tumor tissue, insufficient penetration will yield an ineffective therapy. Many new chemotherapeutic agents have been developed and might also be administered by local polymeric delivery. These drugs include *carmustine*, *paclitaxel*, *5-fluoroacil* (5-FU), and *methotrexate* (MTX). There is a need to analyze their transport mechanisms in brain tumor.

A related issue is the use of antiangiogenic agents to enhance the performance of chemotherapy. It has been hypothesized that this therapy could renormalize the tumor vasculature and, hence, improving the localization of the drug (3). This is achieved by increasing the drug convection within the tumor and decreasing the fluid convection out of the tumor margin (3). However, this concept needs to be further explored for the case of brain tumor, especially when surgery is performed.

To address these questions, a simulation analysis has been performed. This analysis has the advantages of being able to decouple and isolate different aspects of drug transport. Thus, we are able to elucidate (a) which chemotherapeutic agent is more favorable from a transport perspective, and (b) how the antiangiogenic agents could enhance the overall therapy. In addition, recent advances in patient-specific imaging techniques, e.g. magnetic resonance images (MRI) and computed tomography (CT), allow the extraction of brain tissue geometry as well as precise tumor size and location. Here, the simulation utilizes a three-dimensional geometry constructed from MRI of a brain tumor patient so that the possible effect of brain fluid flow can be examined.

Simulation and Mathematical Model

Patient-specific Model Geometry

A MRI of a brain tumor (courtesy of Brain and Spine Clinics, Gleaneagles Hospital, Singapore) was reconstructed by Mimics 10 (Materialise Inc., 2006). This technique is able to reconstruct the

brain geometry with a precision of +/- 3 mm (Fig. 1a). The tumor volume was 12.8 cc, giving an equivalent spherical mean radius (R) of 14.5 mm. The tumor was surgically removed, leaving a cavity in the core and a surrounding residual tumor with an average thickness (L) of 2.3 mm. Subsequently, eight wafers containing drug were inserted into the open cavity. Each is 14 mm in diameter and 1mm thick in thickness. The wafers are held in place by surgical cellulose (Surgicel). This is visualized in Fig. 1b.

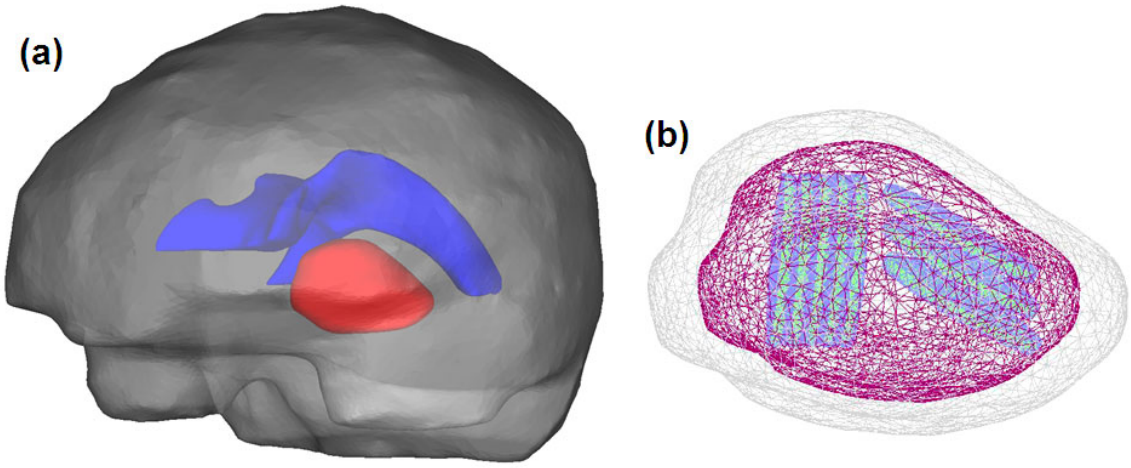

Fig. 1. (a) The model geometry used from a brain tumor patient, showing the presence of: ventricle (shown in blue), tumor (red) located in temporal lobe, and remaining normal brain tissue. (b) The 3D treatment domain with eight wafers containing drug (light green with blue line), cavity (dark red), and remnant tumor (gray).

Transport Model

The transport of interstitial fluid in the brain is described by coupling the modified continuity and momentum equations for fluid flow in a porous medium (4). The interstitial fluid is assumed to be water at 37 ºC. Table I provides the baseline values of parameters related to the flow. The continuity equation for incompressible interstitial fluid in the brain tissue is:

$$\nabla \cdot \mathbf{v} = F_{\mathrm{V}} \tag{1}$$

where $\mathbf{v}$ is superficial fluid velocity vector and F_{V} is the rate of fluid gain from the capillary blood flow per unit volume of tissue. Fluid removal by the lymphatic system is not included because brain tissue lacks a well defined lymphatic system. The fluid gain is assumed to be a non-uniformly distributed source, depending on the pressure difference between blood vessels and interstitial fluid. The constitutive equation for F_{V} follows Starling's law (5):

$$F_{\mathrm{V}} = L_{\mathrm{p}}\left(\frac{S}{V}\right)\left[p_{\mathrm{V}} - p_{\mathrm{i}} - \sigma\left(\pi_{\mathrm{V}} - \pi_{\mathrm{i}}\right)\right] \tag{2}$$

where L_{p} is hydraulic conductivity of the microvascular wall, p_{V} is vascular pressure, p_{i} is interstitial fluid pressure, $\frac{S}{V}$ is available exchange area of the blood vessels per unit volume of tissue, σ is the osmotic reflection coefficient for plasma proteins, and π_{V} and π_{i} are osmotic pressures of blood plasma and interstitial fluid, respectively.

The brain tissue is assumed to be a rigid porous medium. The steady-state momentum equation for fluid flow through tissue is assumed to be:

$$-\nabla p_{\mathrm{i}} + \mu\nabla^2\mathbf{v} - \left(\frac{\mu}{K}\right)\mathbf{v} - \rho\mathbf{v}\cdot\nabla\mathbf{v} = 0 \tag{4}$$

where ρ and μ are density and viscosity of the interstitial fluid and K is the Darcy permeability of the tissue.

The dimensionless forms of the equations of continuity and motion are then as follows:

$$\tilde{\nabla}\cdot\tilde{\mathbf{v}} = \widetilde{F_{\mathrm{v}}} \tag{5}$$

$$-\frac{\left(p_{\mathrm{ventricle}} - p_{\mathrm{outer}}\right)}{\rho v_{\mathrm{s}}^{\,2}}\tilde{\nabla}\widetilde{p_{\mathrm{i}}} + \frac{1}{\mathrm{Re}}\tilde{\nabla}^2\tilde{\mathbf{v}} - \frac{1}{\mathrm{Re}}\left(\frac{L_{\mathrm{brain}}^{\,2}}{K}\right)\tilde{\mathbf{v}} - \tilde{\mathbf{v}}\cdot\tilde{\nabla}\tilde{\mathbf{v}} = 0 \tag{6}$$

where $\tilde{\nabla} = L_{\mathrm{brain}}\nabla$ and L_{brain} is the mean radius of the brain, i.e. 70 mm, which has been chosen as the characteristic length scale), $\tilde{\mathbf{v}} = \mathbf{v}/v_{\mathrm{s}}$ ($v_{\mathrm{s}} = \left(K/\mu\right)\left(p_{\mathrm{ventricle}} - p_{\mathrm{outer}}\right)/L_{\mathrm{brain}} = 1\times10^{-7}$ m/s is the velocity scale), $\widetilde{p_{\mathrm{i}}} = \left(p_{\mathrm{i}} - p_{\mathrm{outer}}\right)/\left(p_{\mathrm{ventricle}} - p_{\mathrm{outer}}\right)$, and $\mathrm{Re} = \rho L_{\mathrm{brain}} v_{\mathrm{s}}/\mu$ is Reynolds number. Insertion of parameter values from Table I leads to the conclusion that Eq. 6 can be further simplified to:

$$\tilde{\mathbf{v}} = -\tilde{\nabla}\widetilde{p_{\mathrm{i}}} \tag{7}$$

Table I. Interstitial Fluid-related Parameter Values

Parameter		Cavity	Remnant Tumor	Normal Tissue
ρ	Density of the interstitial fluid (kg/m^3)	1,000 [7]		
μ	Viscosity of the interstitial fluid (Pa-s)	7×10^{-4} [7]		
p_{v}	Vascular pressure (Pa)	N/A	4,610 [6]	
S/V	Blood vessel exchange area (m^{-1})	N/A	20,000 [5]	7,000 [5]
π_{v}	Vascular osmotic pressure (Pa)	N/A	3,440 [12]	
π_{i}	Interstitial osmotic pressure (Pa)	N/A	1,110 [5]	740 [5]
σ	Osmotic reflection coefficient of plasma	N/A	0.82 [5]	0.91 [5]
L_{p}	Hydraulic conductivity (m/Pa/s)	N/A	1.1×10^{-12}	1.4×10^{-13}
K	Darcy's permeability (m^2)	1×10^{-11}	6.4×10^{-14}	6.4×10^{-15}

In the tissue, drug is always present in the two different forms: free and bound; the latter is usually not subject to metabolism (8). Furthermore, brain tissue consists of three phases: interstitial/extracellular space (ECS), intracellular space (ICS), and cell membrane (CM) (9-11). Both forms of drug are distributed between these three phases and can be expressed as the following:

$$C = \alpha C_{\mathrm{i}} + \beta C_{\mathrm{c}} + \left(1-\alpha-\beta\right)C_{\mathrm{m}} \tag{8}$$

$$B = \alpha B_{\mathrm{i}} + \beta B_{\mathrm{c}} + \left(1-\alpha-\beta\right)B_{\mathrm{m}} \tag{9}$$

where C is the free drug concentration per total brain volume; C_{i}, C_{c}, and C_{m} are the free drug concentrations per unit volume in the interstitial, intracellular, and membrane spaces; while α and β are the volume fractions of the interstitial and cellular spaces. The definition of bound drug is analogous to that for the free drug: B is the free drug concentration per total brain volume; B_{i}, B_{c}, and B_{m} are the bound drug concentrations per unit volume in the interstitial, intracellular, and membrane spaces. It is further assumed that the drug is neither eliminated nor bound in the membrane phase ($B_{\mathrm{m}} = 0$).

In tissue, drug availability is dependent on the rates of transport (diffusion and convection), elimination (via blood capillaries and metabolism/degradation), and local binding (9-11). In interstitial phase, the protein/fat-bound drug is assumed to be locally immobilized as it tends to immediately interact with cell/membrane surfaces due to its lipophilicity; therefore, only unbound drug is available for transport (8). Thus, the drug conservation equation, to be coupled to the flow equations, can be described as follows (9-11):

$$\frac{\partial C}{\partial t} = \alpha D_{\mathrm{i}} \nabla^2 C_{\mathrm{i}} - \nabla \cdot \left(\mathbf{v} C_{\mathrm{i}} \right) - \alpha k_{\mathrm{bbb}} C_{\mathrm{i}} - \beta k_{\mathrm{e}} C_{\mathrm{c}} - \frac{\partial B}{\partial t} \qquad (10)$$

where t is time, D_{i} is drug diffusivity in the interstitial space, k_{bbb} is the first-order elimination constant for drug transport through the BBB, and k_{e} is the enzymatic/non-enzymatic elimination constant due to metabolism/degradation. Table II depicts all parameter values related to the drug.

There are several assumptions made to simplify the drug transport equation as the following: (i) the free drug concentrations in interstitial (C_{i}) and intracellular phase (C_{c}) are directly proportional to those of bound drug (B_{i} and B_{c}), respectively, so that $K_{\mathrm{i}} = B_{\mathrm{i}}/C_{\mathrm{i}}$ and $K_{\mathrm{c}} = B_{\mathrm{c}}/C_{\mathrm{c}}$ where K_{i} and K_{c} are binding constant between bound and free drug in interstitial and intracellular space, respectively; and, (ii) while the membrane phase is inert, local equilibrium is present between interstitial, intracellular, and membrane phases so that $P_{\mathrm{c/i}} = C_{\mathrm{c}}/C_{\mathrm{i}}$ and $P_{\mathrm{m/i}} = C_{\mathrm{m}}/C_{\mathrm{i}}$, where $P_{\mathrm{c/i}}$ is partition coefficient between intracellular and interstitial space, while $P_{\mathrm{m/i}}$ is partition coefficient between cell membrane and interstitial phase. Note that, with these assumptions and transport data from Table II, the total concentration (C) becomes proportional to the concentration in the interstitial phase (C_{i}): $C = nC_{\mathrm{i}}$, where n is a constant.

Table II. Drug-related parameter values

Parameter		BCNU	Taxol	5-FU	MTX
M_{w}	Molecular weight (kg/kmol)	214.06	853.9	130.08	454.44
$C_{\mathrm{i,eff}}$	Effective concentration in interstitial phase (kg/m3)	1.3E-03[11]	7.6E-04[11]	2.6E-04[16]	2.7E-02[16]
$P_{\mathrm{c/i}}$	Partition coefficient between cellular and interstitial phase	1[10]	1[10]	1[10]	1[10]
$P_{\mathrm{m/i}}$	Partition coefficient between membrane and interstitial phase	10.3[10]	3162.3[11]	0.1[13]	0.01[13]
K_{i}, K_{c}	Binding constant between free and bound drugs in interstitial and cellular phase (assume K_{i}=K_{c})	5[10]	5.1[12]	0.1[14]	0.7[15]
D_{i}	Diffusion coefficient in interstitial phase (m^2/s)	1.5E-09[10]	9.0E-10[11]	1.2E-09[13]	5.3E-10[13]
k_{bbb}	Drug elimination to blood capillaries (1/s)	1.4E-02[10]	1.4E-04[11]	1.8E-02[13]	2.8E-04[13]
k_{e}	Drug elimination due to enzymatic/non-enzymatic reactions (1/s)	1.1E-04[10]	6.8E-07[11]	5.6E-04[13]	1.5E-04[13]

Furthermore, the convection term, i.e. $\alpha \nabla \cdot \left(\mathbf{v} C_{\mathrm{i}} \right)$, is comprised of two sub-terms: first containing the gradient of concentration is the usual convective term ($\alpha \mathbf{v} \cdot \nabla C_{\mathrm{i}}$), while the second containing the gradient of fluid velocity is the dilution term ($\alpha C_{\mathrm{i}} \nabla \cdot \mathbf{v}$). The latter can be simplified by Eq. 1 to become a sort of first-order elimination term, i.e. $\alpha F_{\mathrm{v}} C_{\mathrm{i}}$. Finally, the drug conservation equation becomes as follows:

$$\frac{\partial C_{\mathrm{i}}}{\partial t}=\left(\frac{\alpha}{\alpha^{*}}\right)D_{\mathrm{i}}\nabla^{2}C_{\mathrm{i}}-\left(\frac{1}{\alpha^{*}}\right)\mathbf{v}\cdot\nabla C_{\mathrm{i}}-\left(\frac{\alpha k_{\mathrm{bbb}}+\beta k_{\mathrm{e}}+\alpha F_{\mathrm{v}}}{\alpha^{*}}\right)C_{\mathrm{i}} \tag{11}$$

where $\alpha^{*}=\alpha\left(1+K_{\mathrm{i}}\right)+\beta P_{\mathrm{c/i}}\left(1+K_{\mathrm{c}}\right)+\left(1-\alpha-\beta\right)P_{\mathrm{m/i}}$ acts as a retardation constant for transport due to local binding and cell membrane partitioning. In the simplest form, this equation follows the simple diffusion/convection/reaction equation as follows:

$$\frac{\partial C_{\mathrm{i}}}{\partial t}=D\nabla^{2}C_{\mathrm{i}}-\mathbf{v}^{*}\cdot\nabla C_{\mathrm{i}}-kC_{\mathrm{i}} \tag{12}$$

where $D=\left(\alpha/\alpha^{*}\right)D_{\mathrm{i}}$ is the apparent diffusion coefficient in the brain tissue, $\mathbf{v}^{*}=\mathbf{v}/\alpha^{*}$ is the apparent interstitial fluid velocity vector in the brain tissue, and $k=\left(\alpha k_{\mathrm{bbb}}+\beta k_{\mathrm{e}}+\alpha F_{\mathrm{v}}\right)/\alpha^{*}$ is the apparent first-order elimination constant. In the dimensionless form, Eq. 12 can be rewritten as the following.

$$\frac{\partial\Gamma_{\mathrm{i}}}{\partial\tau}=\tilde{\nabla}^{2}\Gamma_{\mathrm{i}}-\mathrm{Pe}\;\tilde{\mathbf{v}}\tilde{\nabla}\cdot\Gamma_{\mathrm{i}}-\phi^{2}\Gamma_{\mathrm{i}} \tag{13}$$

where $\Gamma_{\mathrm{i}}=C_{\mathrm{i}}/C_{\mathrm{i,eff}}$ is dimensionless interstitial free drug concentration relative to the effective therapeutic concentration ($C_{\mathrm{i,eff}}$), $\tilde{\mathbf{v}}=\mathbf{v}/v_{\mathrm{s}}$ is the dimensionless interstitial fluid velocity, $\mathrm{Pe}=v_{\mathrm{s}}L_{\mathrm{d}}/\alpha^{*}D$ is Peclet number that measures the relative importance of drug convection over diffusion in tissue, $\phi=L_{\mathrm{d}}\sqrt{k/D}$ is Thiele modulus that is the ratio of drug elimination rate to diffusion transport, $L_{\mathrm{d}}=\sqrt{D/k}$ is the diffusion/reaction length scale in the remnant tumor, and $\tau=t/k$ is the dimensionless time relative to the first-order elimination constant in the remnant tumor (k). The role of convection is determined by the magnitude of Pe. Note that $\phi=1$ as we standardize to the remnant tumor; in other domains, these dimensionless values will be different accordingly.

Drug release from the wafers

The drug release from the wafers is assumed to be an ideal constant (zero-order) rate, in which 61.6 mg of drug is released in a period of 30 days. Note that the different release mechanism of the drug is not of primary interest in this study.

With this constant release profile, the drug distribution will reach a quasi-steady state after a certain period of initial time. We are interested to study the penetration at this condition where the treatment prevails for most of the release period. Consequently, the quasi-steady form of Eq. 13 becomes:

$$0=\tilde{\nabla}^{2}\Gamma_{\mathrm{i}}-\mathrm{Pe}\;\tilde{\mathbf{v}}\tilde{\nabla}\cdot\Gamma_{\mathrm{i}}-\phi^{2}\Gamma_{\mathrm{i}} \tag{14}$$

Influence of the antiangiogenic therapy to interstitial transport

It is hypothesized that the influence of antiangiogenic therapy is to normalize the tumor vasculature (3). The normalized vasculature leads to a normalized fluid permeation of fluid from the vessels. This is mathematically modeled as the decrease of the hydraulic conductivity (L_{p}) and the blood vessel density (S/V) in the tumor; both parameters appear together as in the Starling's law, $L_{\mathrm{p}}\left(S/V\right)$ (Eq. 2). In an ideal case, the tumor vasculature can be normalized perfectly (as in the normal tissue), the value will be about 21% (m) of its original value ($L_{\mathrm{p}}\left(S/V\right)\big|_{\mathrm{normalized}}=m\,L_{\mathrm{p}}\left(S/V\right)\big|_{\mathrm{tumor}}$). However, the normalization can rarely be ideal; therefore, this model accounts for the maximum

benefit can be gained from the antiangiogenic therapy.

Results and Discussion

Minimal Interstitial Fluid Flow Changes by Antiangiogenic Treatment

Depending on the physiochemical properties of the drug, the role of convective flow to distribute the drug can be important. Therefore, it is important to understand the behavior of the interstitial fluid flow in the treatment domain, especially to account the influence of the antiangiogenic therapy. This is shown in Fig. 2. It basically shows that there is no significant difference in fluid flow under antiangiogenic therapy. In other words, the effect of the treatment to the interstitial fluid flow in the treatment domain is minimal. With the treatment, the mean interstitial pressure in the remnant tumor decreases minimally from 1,104 to 1,062 Pa while the mean fluid velocity remains at 3.18×10^{-7} m/s, confirming that the interstitial fluid flow is not affected by the treatment. Consequently, the drug distribution will no longer influenced by the treatment. This is because that upon the tumor removal surgery the volume portion of tumor is no longer significant; therefore, any changes related to the tumor permeation would be quite decent. At the same time, this also tells that the treatment might be best when big portion of tumor is still available.

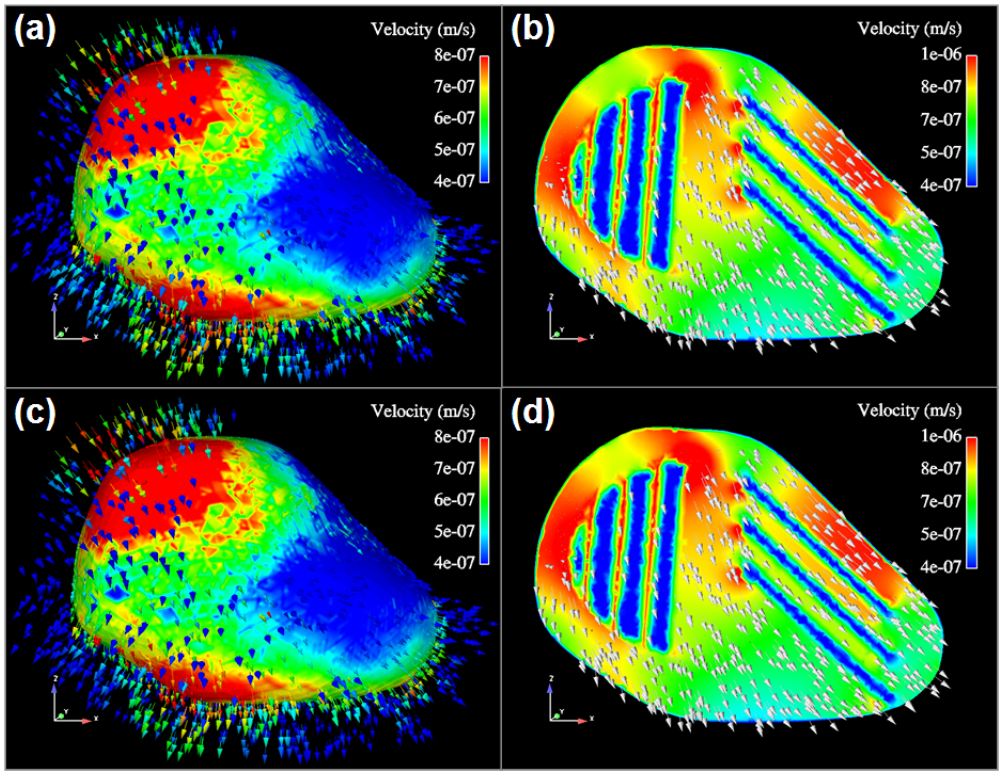

Fig. 2. The fluid flow around and inside the cavity domain for normal case (a and b, respectively) and for the case with antiangiogenic treatment (c and d, respectively). It shows that the antiangiogenic treatment provides minimal effect to the interstitial fluid in the treatment domain. As a result, the treatment will help very minimally the drug distribution to the remnant tumor.

Drug Distribution in the Cavity

While the antiangiogenic therapy might not help the drug distribution to the remnant tumor when surgery is performed, the way drug distributes still depends on its physiochemical properties. Fig. 3 shows the distribution of different chemotherapeutic agents on the cavity surface and its penetration to the remnant tumor (surrounding the cavity). In all cases, the drug concentration profile is along the pressure gradient between the ventricle and the brain periphery – the domain near brain periphery has a relatively higher drug concentration due to the direction of convective flow built by the pressure gradient between the ventricle and the brain periphery.

The physiochemical property of drug in the cavity leads to the availability of the drug on the cavity/remnant tumor interface. Higher drug concentration is observed for the case of *carmustine* and *paclitaxel* than those of 5-FU and MTX. This is because of low Thiele modulus ($\Phi = 0.08$ and 0.05) in the cavity for *carmustine* and *paclitaxel*, respectively. On the other hand, 5-FU and MTX has relatively higher Thiele modulus ($\Phi = 0.17$ and 0.49, respectively). In other words, for the former case (*carmustine* and *paclitaxel*), the elimination is minimal as compared to the drug transport rate by diffusion. In contrast, the elimination is more comparable to the diffusion as for 5-FU and MTX.

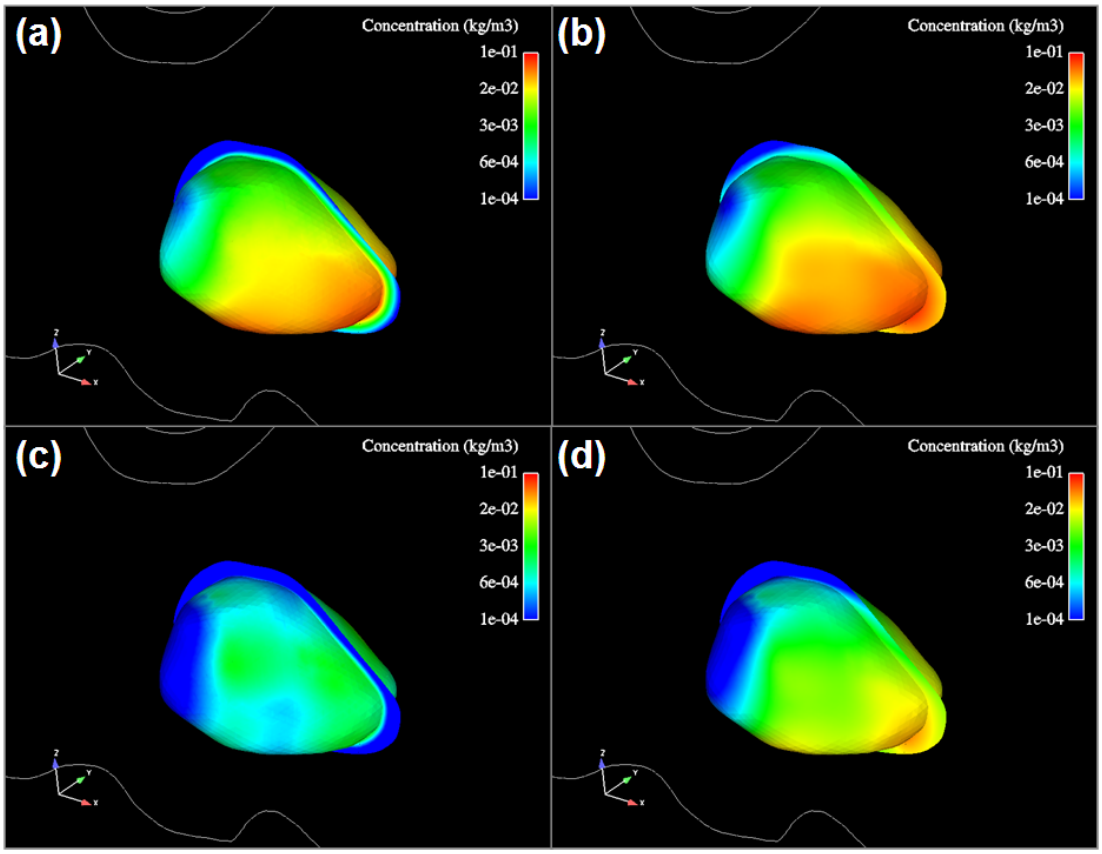

Fig. 3. Drug concentration contour on the surface of cavity and its surrounding remnant tumor (represented by a coronal plane in the middle section of the cavity), showed for four different chemotherapeutic agents: (a) *carmustine*, (b) *paclitaxel*, (c) 5-FU, and (d) MTX.

The convection appears to be more dominant for *paclitaxel* and MTX (Pe = 0.20 and 0.17, respectively) as compared to *carmustine* and 5-FU (Pe = 0.02 for both agents). This is the reason why MTX has higher interface concentration than 5-FU despite the former experiences higher Φ). This also

explains the higher concentration on the interface for *paclitaxel* than *carmustine*. It is also important to note that the direction of convection based on the pressure gradient between the ventricle and brain periphery; thus, the drug will be more concentrated to the right bottom region when the convective transport is more dominant, as in the case of *paclitaxel* and MTX.

Drug penetration to the remnant tumor

Drug penetration to the remnant tumor is based on diffusion and convection. Among four, *paclitaxel* and MTX are the agents which are susceptible to the convective flow (Pe = 0.58 and 0.49, respectively). In contrast, the influence of convective flow can be considered minimal for *carmustine* and 5-FU (Pe = 0.06 for both agents). This suggests that both diffusion and convection are important for *paclitaxel* and MTX while only diffusion is important for *carmustine* and 5-FU. However, drug is also being eliminated when it penetrates the tumor. Hence, the drug penetration is again influenced by its diffusion/reaction length scale (L_d). Higher length scale indicates that drug can penetrate deeper to the tumor, and vice versa. As shown in Fig. 3, relative to the drug concentration on the cavity/remnant tumor interface, *paclitaxel* and MTX (L_d = 1.8 and 0.9 mm, respectively) penetrate farther than *carmustine* and 5-FU (L_d = 0.3 and 0.2 mm, respectively). The limited penetration of the latter two is primarily due to their rapid capillary elimination (high k_{bbb}).

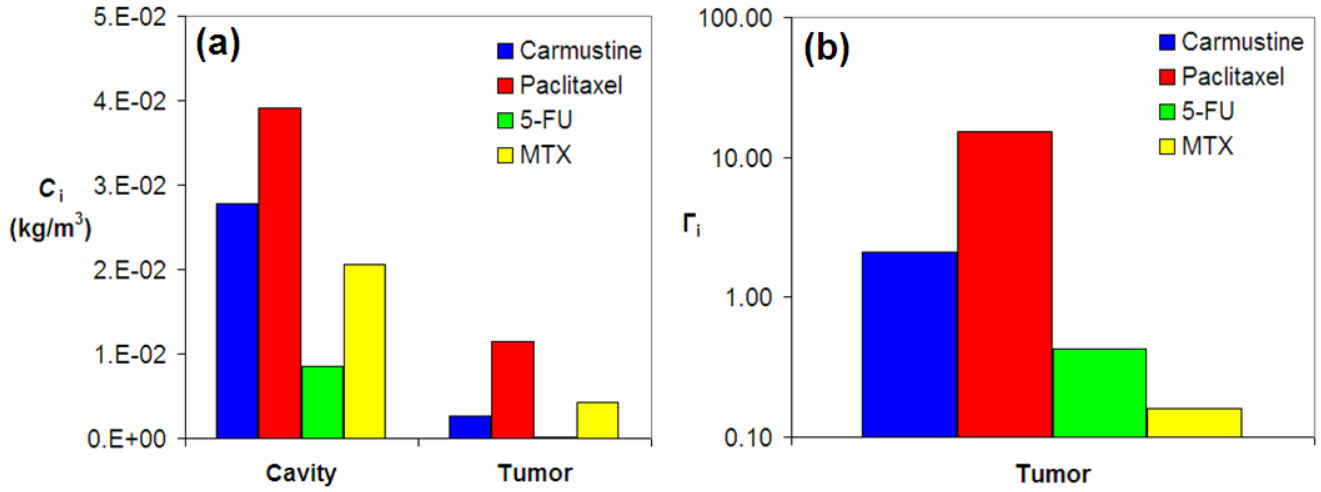

Fig. 4. The availability of each chemotherapeutic agent for a given dosage under constant release (61.6 mg continuously released in 30 days). (a) Shown is the mean concentration of the drug in the cavity and the remnant tumor. (b) Shown relative to the effective concentration in the tumor ($\Gamma_i = C_i / C_{i,eff}$).

The drug availability in the remnant tumor is quantitatively compared by its mean concentration. This is shown in Fig. 4a. In the cavity, the highest concentration is obtained by *paclitaxel*, followed by *carmustine*, MTX, and 5-FU. As discussed previously, this is because of the combination of diffusion and convection relative to elimination in the cavity. In the remnant tumor, *paclitaxel* is still available at the highest concentration. Interestingly, MTX surpasses *carmustine*. This is because, unlike MTX, *carmustine* is carried away significantly by capillary elimination. The availability of 5-FU also suffers due to the significant capillary elimination, and it is shown as the lowest available in the remnant tumor. However, the efficacy of each drug against brain tumor depends on its effective concentration ($C_{i,eff}$). Fig. 4b shows the normalized concentration relative to its

effective concentration in the tumor ($\Gamma_i = C_i / C_{i,eff}$). For the same current dosage, *paclitaxel* again shows it superiority against other agents. The mean concentration in the tumor is about fifteen times of its effective concentration. This is followed by *carmustine*, 5-FU, and MTX, which provides about two, two-fifth, and one-fifth times of its individual effective concentration, respectively. Note that this prevails particularly for the dosage used in this study (61.6 mg of drug constantly released in 30 days). High Γ_i (>1) simply indicates that drug can penetrate well and be available above its effective concentration in the tumor. Consequently, lower dosage might be preferred to avoid any toxicity to the surrounding normal tissue. On the other hand, low Γ_i (<1) suggests the opposite: the drug penetrates poorly and is not available at sufficient concentration in the tumor. Consequently, higher dosage will be required to achieve a satisfactory treatment.

CONCLUSIONS

Clinical Implications

This study shows that the distribution of the drug in the brain tumor treatment relies on its physiochemical properties. Hence, while the therapeutic efficacy against the disease is essential, ones also need to carefully consider the amount of dosage and its release mechanism in order to achieve optimal drug delivery strategy. In this case, computer simulation has shown its advantages to predict the drug distribution for various scenarios. In addition, we predict that the effect of antiangiogenic therapy to enhance drug penetration in the case of brain tumor with resection will be quite minimal.

References

1. H. Brem and P. Gabikian (2001), Biodegradable polymer implants to treat brain tumors Journal of Controlled Release 74:63-67.
2. A.B. Fleming and W.M. Saltzman (2002), Pharmacokinetics of the carmustine implant. Clinical Pharmacokinetics 41:403-419.
3. R.K. Jain, R.T. Tong, L.L. Munn. Effect of vascular normalization by antiangiogenic therapy on interstitial hypertension, peritumor edema, and lymphatic metastasis: Insights from a mathematical model. Cancer Research 67:2729-2735.
4. J.F. Gross and A.S. Popel (1979), Mathematical models of transport phenomena in normal and neoplastic tissue In H.I. Peterson (ed.), Tumor Blood Circulation, CRC Press, Baca Raton, pp. 169-183.
5. L.T. Baxter and R.K. Jain (1989), Transport of fluid and macromolecules in tumors. I. Role of interstitial pressure and convection. Microvascular Research 37:77-104.
6. H.K. Kimelberg (2004), Water homeostasis in the brain: Basic concepts, Neuroscience 120:852-860.
7. R.H. Perry (1997), Perry's Chemical Engineers' Handbook (Ed.), McGraw-Hill, New York, pp. 59-71.
8. D.E. Golan, A.H. Tashjian, E. Armstrong, J.M. Galanter, A.W. Armstrong, R.A. Arnaout, H.S. Rose (2008), Principles of Pharmacology: The Pathophysiologic Basis of Drug Therapy, Lippincot Williams & Wilkins, Baltimore MD, pp. 58-59.
9. A.B. Fleming and W.M. Saltzman (2002), Pharmacokinetics of the *carmustine* implant. Clinical Pharmacokinetics 41:403-419.

10. L.K. Fung, M. Shin, B. Tyler, H. Brem, and W.M. Saltzman (1996), Chemotherapeutic drugs released from polymers: distribution of *1,3-bis(2-chloroethyl)-1-nitrosurea* in the rat brain. Pharmaceutical Research 13:671-682.
11. L.K. Fung, M.G. Ewend, A. Silis, E.P. Sipos, R. Thompson, M. Watts, O.M. Colvin, H. Brem, and W.M. Saltzman (1998), Pharmacokinetics of interstitial delivery of *carmustine*, 4-*hydroperoxycyclophospamide*, and *paclitaxel* from a biodegradable polymer implant in the monkey brain. Cancer Research 58:672-684.
12. H.-J. Kuh, S.H. Jang, M.G. Wientjes, J.L.-S. Au (2000), Computational Model of Intracellular Pharmacokinetics of Paclitaxel. The Journal of Pharmacology and Experimental Therapeutics 293:761-770.
13. W.M. Saltzman and M.L. Radomsky (1991), Drugs released from polymers: diffusion and elimination in brain tissue. Chemical Engineering Science 46:2429-2444.
14. D.S. Wishart, C. Knox, A.C. Guo, S. Shrivastava, M. Hassanali, P. Stothard, Z. Chang, J. Woolsey, (2006) Drug Bank: A comprehensive resource for in silico drug discovery and exploration, Nucleic Acids Research 34:D668-672.
15. M.B. De Sousa Maia, S. Saivin, E. Chatelut, M.F. Malmary, G. Houin (1996), In vitro and in vivo protein binding of methotrexate assessed by microdialysis, International Journal of Clinical Pharamacology and Therapeutics 34:335:341.
16. C.M. Hand, J.R. Vender, P. Black (1988), Chemotherapy in experimental brain tumor, part 1: In vitro calorimetric MTT assay, Journal of Neuro-Oncologty 36:1-6.